POLITECNICO DI TORINO
Repository ISTITUZIONALE

Design strategies and merit of system parameters for uniform uncompensated links supporting Nyquist-WDM transmission

Original
Design strategies and merit of system parameters for uniform uncompensated links supporting Nyquist-WDM transmission / Curri, V., Carena, A., Arduino, A., Bosco, G., Poggiolini, P., Nespola, A., Forghieri, F.. - In: JOURNAL OF LIGHTWAVE TECHNOLOGY. - ISSN 0733-8724. - STAMPA. - 33:18(2015), pp. 3921-3932. [10.1109/JLT.2015.2447151]

Availability:
This version is available at: 11583/2646780 since: 2016-08-31T14:25:54Z

Publisher:
Institute of Electrical and Electronics Engineers Inc.

Published
DOI:10.1109/JLT.2015.2447151

Terms of use:

This article is made available under terms and conditions as specified in the corresponding bibliographic description in the repository

Publisher copyright
IEEE postprint/Author's Accepted Manuscript

©2015 IEEE. Personal use of this material is permitted. Permission from IEEE must be obtained for all other uses, in any current or future media, including reprinting/republishing this material for advertising or promotional purposes, creating new collecting works, for resale or lists, or reuse of any copyrighted component of this work in other works.

(Article begins on next page)

26 November 2026

Software-defined Radio Experimental Setup for Multi-Antenna Spectrum Sensing Algorithms

Daniel Gaetano Riviello*, Giusi Alfano†
*CNR-IEIIT, Consiglio Nazionale delle Ricerche, Torino, Italy
daniel.riviello@cnr.it
†DIEI, University of Cassino and Southern Lazio, Cassino, Italy
giuseppa.alfano@unicas.it

***Abstract*—Spectrum Sensing (SS) will play a pivotal role in 6G Cognitive Radio Networks (CRN), in which unlicensed users could dynamically use the spectrum and perform opportunistic transmission, while avoiding interference. In this paper, we focus on multiple-antenna SS and we compute the performance of three schemes, the Roy's Largest Root Test (RLRT), the Generalized Likelihood Ratio Test (GLRT), and the Energy Detector (ED), for different values of false alarm probability and signal-to-noise ratio, and fixed number of sensors at the secondary user receiver, equal to 4. In order to assess the performance of SS schemes in a real environment, we set up a software-defined radio (SDR) experimental testbed by using Universal Software Radio Peripherals (USRPs) for primary user signal transmission and secondary user data acquisition. Results of the SDR setup, shown in terms of Receiving Operating Characteristic (ROC) curve and performance curve, are compared against simulated data, confirm the performance superiority of RLRT over ED and GLRT also in a real environment.**

***Index Terms*—Software Defined Radio; 6G CRN; Spectrum Sensing; RLRT; GLRT; URSP; Random matrix eigenvalues;**

I. Introduction

THE idea of Cognitive Radios Networking (CRN) [1], introduced to alleviate the scarcity of spectral resources by facilitating the coexistence between unlicensed and licensed users [2], while avoiding interference, is expected to be largely exploited in upcoming 6G communication networks. A fundamental task of CRN is the ability of discriminating the presence of a primary user/signal (busy channel) against background noise (clear channel). The investigation of efficient Spectrum Sensing (SS) strategies has been, therefore, among the main goals of the wireless communications community during the last two decades [3]–[5]. This work is devoted to measurement-based analysis of some among the most frequently adopted SS schemes, whose test statistics to discriminate between presence vs. absence of a primary signal on the channel depend on spectral statistics of the collected data sample covariance matrix (see e.g., [6]–[8], and [9, and references therein]), by means of a multiple-antenna equipped receiver. Such test statistics are, in turn, devised by following classical approaches of estimation theory (e.g., resorting to Likelihood Ratio based criteria [10], or relying on the law of the Largest Latent Root of the sample covariance [11]), or based on natural heuristics (e.g. based on the change in values of the received power [12], depending on the presence of a primary signal).

Software-Defined Radio (SDR) platforms are tightly related to CRN, the former providing a flexible hardware, reconfigurable based on software inputs, suitable to implement the dynamic capabilities of the latter. Universal Software Radio Peripheral (USRP), in particular, as a SDR platform, is able to provide the real-time signal processing and reconfiguration, critical for CRN featured functions, such as SS, dynamic spectrum access, and interference management. A wise combination of CRNs and SDRs paves therefore the way for more efficient and intelligent wireless communication systems. Several testbeds and experimental setups have been carried out in literature, especially related to the well-know Energy Detector (ED) [12]–[14] and cyclostationary feature-based detectors [15]. In this paper, measured vs. simulated data based performance of widely adopted eigenvalue-based SS schemes, namely the Generalized Likelihood Ratio Test (GLRT) [10], and the classical Roy's Largest Root Test (RLRT) [11] are considered, as well as the aforementioned ED for comparison. Actual data samples are generated and acquired in a USRP-based experimental setup.

Analytical performance analysis of the mentioned tests has been carried out under various assumptions on the channel fading, the number of receive antenna and of collected snapshots. Random Matrix Theory (RMT) has been exploited for the direct computation of the probability of erroneously sensing the presence of a primary user when it is in fact absent, and, respectively, of the probability of detecting a primary signal actually present on the channel. Two main, and complementary, approaches are usually adopted: indeed, either a finite-sized regime (see e.g. [16, and references therein]), where the number of receive antenna and the number of collected channel samples are both finite, or a large-system [17] analysis, where the focus is on the ratio between the numbers of involved sensors and samples, and on the corresponding performance scaling, are investigated. While the first approach has the privilege to offer exact results, often, corresponding expressions are too involved, to gain insights into system design guidelines; therefore, the resort to the asymptotic approach is quite popular.

The work is articulated as follows: Sec. II develops the system model and the sensing schemes description. In Sec. III, performance computation, based on an asymptotic approach, is detailed. Experimental setup and numerical results are reported in Section IV, while Sec. V concludes the work.

Notation: Throughout the paper, we denote vectors and matrices with boldface lowercase and uppercase letters, respectively. A hat on the variable denotes an estimated quantity (either numerically or measurements-based). By $\mathrm{E}[\cdot]$ we denote the statistical expectation, while $\mathcal{U}(N)$, with positive integer N, stands for the unitary group of matrices of size N. $||\cdot||$ denotes the Euclidean norm of a vector, $\|\cdot\|_F$ the Frobenius norm of a matrix, while by $\mathrm{tr}(\cdot)$ we denote the trace of a square matrix. For matrices and vectors, $(\cdot)^H$ indicates the conjugate-transpose. Finally, $|\cdot|$ is the determinant of a square matrix.

II. System Model and Spectrum Sensing Schemes

We focus on a SS setting, where a receiver equipped with K antennas collects N time samples from each antenna. We denote by $\mathbf{y}(n) = [y_1(n), \ldots, y_K(n)]^T$ the $K \times 1$ received vector at time $n \in \{1, \ldots, N\}$, with generic entry $y_k(n)$ denoting the discrete baseband complex sample at the k-th receive antenna.

Under $\mathcal{H}_0$, namely in absence of a primary signal, $y_k(n)$ is a vector of complex Gaussian noise samples with zero mean and variance σ_v^2

$$\mathbf{y}(n)|_{\mathcal{H}_0} = \mathbf{v}(n) \tag{1}$$

where $\mathbf{v}(n) \sim \mathcal{N}_{\mathbb{C}}(\mathbf{0}_{K\times 1}, \sigma_v^2 \mathbf{I}_{K\times K})$. Under $\mathcal{H}_1$, instead, both primary signal and noise are present, therefore

$$\mathbf{y}(n)|_{\mathcal{H}_1} = \mathbf{x}(n) + \mathbf{v}(n) = \mathbf{h}s(n) + \mathbf{v}(n) \tag{2}$$

where $s(n)$ is the transmitted signal sample, modeled without loss of generality as Gaussian distributed with zero mean and variance σ_s^2, while $\mathbf{h}$ is the $K \times 1$ unknown complex channel vector, affected by Rayleigh flat fading. The channel is assumed to be memoryless, and constant during the detection time, i.e., block fading is assumed. Under $\mathcal{H}_1$, we define the Signal-to-Noise Ratio (SNR) at the receiver as

$$\rho \triangleq \frac{\mathrm{E}\,\|\mathbf{x}(n)\|^2}{\mathrm{E}\,\|\mathbf{v}(n)\|^2} = \frac{\sigma_s^2}{\sigma_v^2}\frac{\|\mathbf{h}\|^2}{K}. \tag{3}$$

The detector collects the received samples in the $K \times N$ matrix

$$\mathbf{Y} \triangleq [\mathbf{y}(1) \ldots \mathbf{y}(N)] = \mathbf{h}\mathbf{s} + \mathbf{V} \tag{4}$$

where $\mathbf{s} \triangleq [s(1) \ldots s(N)]$ is a $1 \times N$ signal vector and $\mathbf{V} \triangleq [\mathbf{v}(1) \ldots \mathbf{v}(N)]$ is a $K \times N$ noise matrix. The sample covariance matrix $\mathbf{R}$ of the received samples is therefore given by

$$\mathbf{R} \triangleq \frac{1}{N}\mathbf{Y}\mathbf{Y}^H. \tag{5}$$

In our subsequent analysis, we shall make reference to the spectral decomposition of $\mathbf{R} = \mathbf{U}\mathbf{\Lambda}\mathbf{U}^H$, with $\mathbf{U}$ denoting the random unitary matrix of the eigenvectors, and $\mathbf{\Lambda}$ the diagonal matrix of the random eigenvalues, whose largest is denoted by $\lambda_{\max}$ throughout the work.

The test statistic employed by the detector to discriminate between the null hypothesis $\mathcal{H}_0$ and the presence of primary signal $\mathcal{H}_1$ is denoted by T; to take a decision, the detector compares it against a pre-defined threshold t: if $T > t$ it decides for $\mathcal{H}_1$, otherwise for $\mathcal{H}_0$. As a consequence, the *probability of false alarm* P_{fa} is defined as

$$P_{\mathrm{fa}} = \Pr(T > t|\mathcal{H}_0) \tag{6}$$

and the *detection probability* as

$$P_{\mathrm{d}} = \Pr(T > t|\mathcal{H}_1). \tag{7}$$

Hereinafter, we detail the three SS schemes exploited in the experimental setups. The first one, the ED, exploits the difference in energy levels corresponding to the two alternative scenarios of presence vs. absence of primary signal. The remaining two schemes are based on classical estimation-theoretic criteria, and involve also the largest eigenvalue of the sample covariance matrix of the collected data.

A. Energy Detector

The test statistic T_{ED} computes the average energy of the received signal over the N collected samples, normalized by the noise variance σ_v^2, namely

$$T_{\mathrm{ED}} = \frac{1}{KN\sigma_v^2}\sum_{k=1}^{K}\sum_{n=1}^{N}|y_k(n)|^2 = \frac{\|\mathbf{Y}\|_F^2}{KN\sigma_v^2}. \tag{8}$$

Note that, since, by definition of Frobenius norm, $\|\mathbf{Y}\|_F^2 = \mathrm{tr}(\mathbf{Y}\mathbf{Y}^H)$, T_{ED} can be expressed in terms of the spectrum of the sample covariance, as follows

$$T_{\mathrm{ED}} = \frac{\mathrm{tr}(\mathbf{R})}{K\sigma_v^2} = \frac{\sum_{i=1}^{K}\lambda_i}{K\sigma_v^2}. \tag{9}$$

For this test, since the law of the normalized trace $\mathrm{T}_n = \mathrm{tr}(\mathbf{R})/K$ can be found, e.g. in [19, Eq.(8)] as

$$f_{\mathrm{T}_n}(x) = \frac{K^{KN}}{(KN-1)!}x^{KN-1}e^{-Kx}, \tag{10}$$

the corresponding P_{fa} can be written as

$$P_{\mathrm{fa}} = \Pr(\mathrm{T}_n > \sigma_v^2 t|\mathcal{H}_0) = e^{-K\sigma_v^2 t}\sum_{\ell=0}^{KN-1}\frac{(K\sigma_v^2 t)^\ell}{\ell!}. \tag{11}$$

B. GLRT statistics

In case of GLRT-based SS, the test statistic, derived applying the GLR criterion to our detection problem, reads as

$$T_{\mathrm{GLRT}} \triangleq \frac{\lambda_{\max}}{\frac{1}{K}\mathrm{tr}(\mathbf{R})}, \tag{12}$$

whose exact[1] pdf and CDF for finite values of K and N have been provided in [19], [20], while approximations thereof appeared in several works[2].

[1]Notice that, even though the correlation between $\lambda_{\max}$ and the normalized trace is intractable, as observed in [18], (12) and (9) are statistically independent.

[2]for finite-size settings, we refer the interested reader to the references provided in the already cited works [19], [20], while a thorough analysis of the literature in the asymptotic case can be found, e.g. in [10], [21].

C. RLRT

Roy's test exploits as test statistics the largest eigenvalue of the sample covariance, normalized by the noise variance. Since, therefore,

$$T_{\mathrm{RLRT}} \triangleq \frac{\lambda_{\max}}{\sigma_v^2}, \tag{13}$$

P_{fa} can be immediately computed, for this sensing scheme, as

$$P_{\mathrm{fa}} = 1 - \Pr(\lambda_{\max} < \sigma_v^2 t | \mathcal{H}_0) = 1 - \frac{|\mathbf{\Phi}(\sigma_v^2 t)|}{\mathcal{C}_{K,N}}, \tag{14}$$

with $\mathcal{C}_{K,N} = \prod_{\ell=1}^{K} (N-\ell)!(K-\ell)!$, and where

$$[\mathbf{\Phi}(x)]_{i,j} = (N+K+i+j-2)! \left(1 - e^{-x} \sum_{k=0}^{N+K+i+j-2} \frac{x^k}{k!}\right).$$

Let us recall that, under $\mathcal{H}_0$, the CDF of $\lambda_{\max}$ is provided in [24, Corollary 2], while, under $\mathcal{H}_1$, it assumes the expression derived in [25].

III. Performance Computation

Receiver Operating Characteristics (ROC) are computed based on the value of the main figures of merit, namely the P_{fa} and the P_{d}, for a given threshold t, whose setting is detailed in this Section.

ED performance is computed according to the characterization of T_{ED} provided in the previous Section. In order to assess the analytical performance of RLRT and GLRT, instead, we resort to an asymptotic approach, assuming K, N to grow large at the same rate, and exploiting known results on the spectral behavior of the sample covariance matrix $\mathbf{R}$ in the large-system regime. Specifically, let us define the *aspect ratio* of the random matrix $\mathbf{R}$ as

$$c \triangleq \frac{K}{N} \tag{15}$$

for $K, N \to \infty$ and $K \ll N$, and the following parameters, depending on c, as

$$\mu_+(c) \triangleq \left(c^{1/2} + 1\right)^2 \tag{16}$$

$$\xi_+(c) \triangleq \left(c^{1/2} + 1\right)\left(c^{-1/2} + 1\right)^{1/3}. \tag{17}$$

Nowadays very well known results include almost sure convergence of the largest eigenvalue [23], namely

$$\lambda_{\max} \xrightarrow{a.s.} \sigma_v^2 \mu_+(c), \tag{18}$$

and the convergence in distribution of the scaled and normalized largest eigenvalue, i.e.

$$N^{2/3} \frac{\lambda_1 - \sigma_v^2 \mu_+(c)}{\sigma_v^2 \xi_+(c)} \tag{19}$$

to a random variable distributed according to a second order Tracy-Widom distribution (TW2), whose CDF for the Gaussian Unitary Ensembles (GUE) is explicitly given by:

$$F_{TW2}(x) = \exp\left(-\int_x^\infty (s-x) q^2(s)\, ds\right) \tag{20}$$

where $q(s)$ is the unique solution to the Painlevé II differential equation

$$q''(s) = s q(s) + 2q^3(s) \tag{21}$$

satisfying the boundary condition

$$q(s) \sim \mathrm{Ai}(s), \quad s \to +\infty \tag{22}$$

where $\mathrm{Ai}(s)$ denotes the Airy special function, one of the two linearly independent solutions to the following differential equation:

$$z''(w) - w z(w) = 0 \tag{23}$$

In presence of a primary signal, the asymptotical value and limiting distribution of the largest eigenvalue of the sample covariance matrix $\mathbf{R}$ can be characterized, exploiting classical results on the so-called *spiked models* of random matrices, by defining the quantities

$$\tau_1 = K\rho + 1, \tag{24}$$

$$\mu_s(\tau_1, c) \triangleq \tau_1 \left(1 + \frac{c}{\tau_1 - 1}\right) \tag{25}$$

and

$$\xi_s(\tau_1, c) \triangleq \tau_1 \sqrt{1 - \frac{c}{(\tau_1 - 1)^2}}. \tag{26}$$

Under $\mathcal{H}_1$, then, undergoing a phase transition in dependence of the relative strength of the primary signal, (see [26])

$$\begin{cases} \lambda_{\max} \xrightarrow{a.s.} \sigma_v^2 \mu_+(c), & \text{if } \tau_1 \le 1 + c^{1/2} \\ \lambda_{\max} \xrightarrow{a.s.} \sigma_v^2 \mu_s(\tau_1, c), & \text{if } \tau_1 > 1 + c^{1/2}. \end{cases} \tag{27}$$

The phase transition threshold therefore impacts on the identifiability of a signal with RLRT or GRLT, which can take place only if

$$\tau_1 > 1 + c^{1/2} \tag{28}$$

After phase transition, namely in case signals are actually identifiable, the scaled and normalized largest eigenvalue converges in distribution to a standard real Gaussian random variable [22], i.e.

$$N^{1/2} \frac{\lambda_1 - \sigma_v^2 \mu_s(\tau_1, c)}{\sigma_v^2 \xi_s(\tau_1, c)} \to \mathcal{N}(0,1), \qquad \text{if } \tau_1 > 1 + c^{1/2}. \tag{29}$$

As a consequence of the recalled convergence results for the largest eigenvalue, it turns out (cite appropriate refs or thesis) that an approximate expression for the threshold of RLRT, for a given tolerated false-alarme rate of α, is

$$t_{RLRT}(\alpha) \approx \mu + F_{TW2}^{-1}(1-\alpha)\xi \tag{30}$$

where F_{TW2}^{-1} is the inverse of the TW2 CDF (20). We also remark that, for single signal detection, the presence of a phase transition phenomenon for detectability under the alternate hypothesis we just discussed, can be explicitly formulated in terms of a critical detection threshold, depending on the SNR as

$$\rho_{Crit} = \frac{1}{\sqrt{KN}} \tag{31}$$



Fig. 1. SDR experimental setup composed of a host computer equipped with MATLAB, a USRP X310 transmitter, and a USRP X410 multi-antenna receiver.



Fig. 2. Ettus Research USRP X310 and NI Ettus USRP X410 on the right.

As to the GLRT, an effective approximation for its P_{fa} can be found in [17]:

$$\Pr\left[\frac{T_{GLRT}-\mu}{\xi} < s\right] \approx F_{TW2}(s) - \frac{1}{2NK}\left(\frac{\mu}{\xi}\right)^2 F''_{TW2}(s), \tag{32}$$

an equation that can be numerically inverted in efficient way, to find the required threshold $t_{GLRT}(\alpha)$.

IV. Experimental Setup and Numerical Results

Fig. 1 and 2 show the SDR experimental setup in which the multi-antenna SS algorithms have been tested and validated through over-the-air signal transmission and acquisition, and subsequent data processing and performance evaluation. The setup is composed of three main components:

- a host computer, the SiComputer Extrema Workstations W200, equipped with CPU Intel Core i9-14900K, 3200 MHz and 24 cores, 64 GB DDR4 RAM, and a Mellanox ConnectX-5 100 Gbps Ethernet adapter. The installed SDR software is MATLAB R2024b together with the Wireless Testbench support package for NI USRP radios.
- Ettus Research USRP X310, equipped with a Xilinx Kintex-7 FPGA, 2 independent TX/RX channels, able to stream up to 200 MSamples/s per channel. The USRP X310 is used as single antenna transmitter and is connected to to the workstation through a 10 Gbps Ethernet adapter. Notice that there is no external antenna connected to the transmitter, in order to obtain sufficiently low SNR levels, suitable to test the SS schemes at hand.
- NI Ettus USRP X410, equipped with a Xilinx Zynq Ultrascale+ ZU28DR RF System on Chip (RFSoC), 4 independent TX/RX channel, able to stream up to 250 MSamples/s per channel. The USRP X410 is used as multi-antenna receiver and is connected to the workstation through the QSFP28 interface to the 100 Gbps Ethernet adapter.

In order to assess the performance of RLRT, ED and RLRT SS schemes, we assumed as primary user signal a single carrier QPSK modulated signal at carrier frequency $f_c = 3.85$ GHz with a baud rate R_s of 1 MBd/s. We used 4 samples per symbol, therefore the USRPs radio have been set to a sample rate $f_s = 4$ Msamples/s. The narrowband choice for the primary signal has been made to ensure a flat fading channel. Given the 4 channels of the USRP X410, $K = 4$, while $N = 20$ samples. Thresholds have been previously computed for several values of P_{fa}, while for ED, it is quite straightforward, for RLRT we used Momar Dieng's MATLAB package "RMLab" [28] which provides the CDF F_{TW2} of the TW2 distribution, we computed the scaling and centering parameters as in (16) and (17), and the we used the bisection method to retrieve the correct threshold t_{RLRT} value for any input P_{fa}. For GLRT we used the routines in [17], which provides the inverted modified distribution of (32). The SDR experiment could be summarized into 3 phases:

1) Noise variance estimation under $\mathcal{H}_0$: in this phase, no transmission occurs and the USRP X410 aquires samples over its 4 channels for a total duration of $T_0 = 4$ s. Under null hypothesis, the Maximum Likelihood estimation of the noise variance σ_v^2 can be written as:
$$\hat{\sigma}_v^2 = \frac{\|\mathbf{Y}|_{\mathcal{H}_0}\|_F^2}{KN}. \tag{33}$$
2) Primary user signal transmission and multi-antenna acquisition under $\mathcal{H}_1$: the USRP X310 is set up to continuously transmit the QPSK modulated signal, and simultaneously the USRP X410 acquires samples under $\mathcal{H}_1$ again for $T_0 = 4$ s. We can estimate the SNR $\hat{\rho}$ at the receiver as:
$$\hat{\rho} = \frac{\|\mathbf{Y}|_{\mathcal{H}_1}\|_F^2}{KN\hat{\sigma}_v^2} - 1 \tag{34}$$
3) Performance evaluation and comparison with simulated data: in the last phase, we process the acquired samples into slots of $N = 20$ samples, and we compute the RLRT, GLRT, and ED test statistics. The results are generated through error counting by means of ROC curves for a specific SNR value, and by mean of P_{d} vs. SNR curve for a specific P_{fa} value. In particular, for fixed P_{fa}, the points of each curve are obtained, from the experimental setup by progressively increasing the transmit gain of 0.5 dB at each step, and repeating the procedure detailed in these three steps. Experimental results are compared against simulated ones, i.e., we perform a parallel Monte Carlo simulation by generating Gaussian samples with signal variance $\tilde{\sigma}_s^2 = \hat{\rho}\,\hat{\sigma}_v^2/\|\mathbf{h}\|^2$ and we apply the same test statistics and metrics evaluation.

ROC curves are reported in Fig. 3 for all three schemes. Nonidealities in the experimental setup (such as interference during noise estimation, quantization noise, etc.) clearly impact on the corresponding performance, which results poorer than the simulated counterparts. Evidently, RLRT outperforms

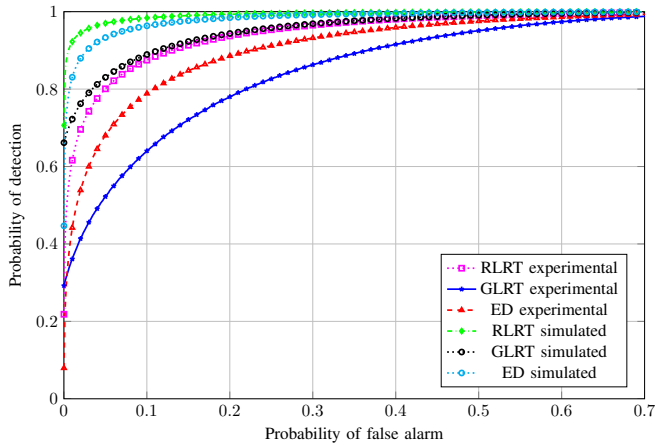

Fig. 3. ROC curve, $N = 20$, $K = 4$, SNR $= -3.42$ dB.

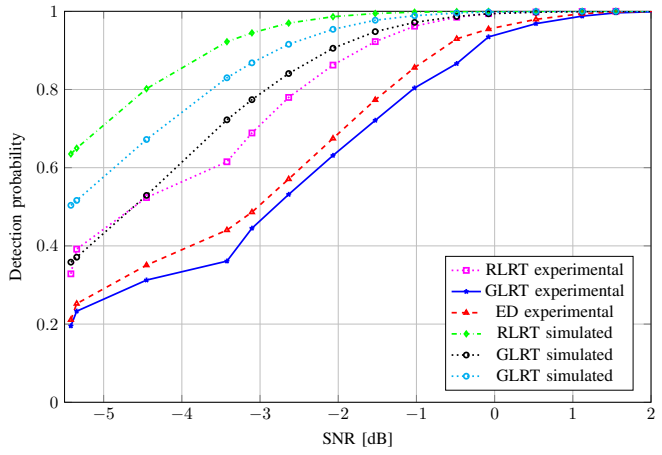

Fig. 4. P_{d} vs. SNR, $N = 20$, $K = 4$, $P_{\mathrm{fa}} = 0.01$.

both ED and GLRT, which is expected to be the least performing sensing scheme, since it is the only blind test with no prior knowledge of the noise variance. The performance curves representing the behavior of the detection probability vs. SNR are drawn in Fig. , for which a very similar behavior of all tests as in Fig. 3 can be observed, as performance ranking among the analyzed algorithms is retained. Specifically, the experimental test statistics, with data acquired through SDR plaforms, require approximately 0.5-1 dB more to achieve the same performance of the simulated ones.

V. Conclusion

A SDR experimental setup for testing the performance of multi-antenna SS algorithms has been built, and the corresponding collected data have been exploited to compute false-alarm and detection probabilities for Energy Detection, GLRT and RLRT, in presence of $K = 4$ receive antennas at the secondary user equipment. Measurement-based performance curves have been contrasted with the results of numerical simulations. Reported curves show an extremely satisfactory match between simulated and real data.

Acknowledgment

The work of Daniel Gaetano Riviello was partially supported by the European Union – NextGenerationEU – National Recovery and Resilience Plan (Piano Nazionale di Ripresa e Resilienza, PNRR) through the Project: “SoBigData.it – Strengthening the Italian RI for Social Mining and Big Data Analytics”, under Grant Prot. IR0000013 – Avviso n. 3264 del 28/12/2021. The work of G. Alfano has been funded by the European Union - NextGenerationEU under the project NRRP RESTART, RESearch and innovation on future Telecommunications systems and networks, to make Italy more smART PE_00000001 - Cascade Call SMART project, with CUP E63C22002040007.

References

[1] J. Mitola, III and G. Q. Maguire, Jr., “Cognitive radio: Making software radios more personal”, *IEEE Personal Communications*, 1999.

[2] A. Ivanov, K. Tonchev, V. Poulkov, and A. Manolova, “Probabilistic spectrum sensing based on feature detection for 6G cognitive radio: a survey,” *IEEE Access*, vol. 9, pp. 116994–117026, Aug. 2021.

[3] A. Kortun, T. Ratnarajah, M. Sellathurai, C. Zhong, and C. B. Papadias, “On the performance of eigenvalue-based cooperative spectrum sensing for cognitive radio,” *IEEE Journal on Selected Topics Signal Processing*, vol. 5, no. , pp. 49–55, Feb. 2011.

[4] P. Salvo Rossi, D. Ciuonzo, and G. Romano, “Orthogonality and Cooperation in Collaborative Spectrum Sensing through MIMO Decision Fusion,” *IEEE Transactions on Wireless Communications*, vol. 12, no. 11, pp. 118–125, Nov. 2013.

[5] Y. Li, W. Zhang, C.-X. Wang, J. Sun, and Y. Liu, “Deep reinforcement learning for dynamic spectrum sensing and aggregation in multi-channel wireless networks,” *IEEE Transactions on Cognitive Communications and Networking* , vol. 6, no. 2, pp. 464–475, June 2020.

[6] F. Penna, R. Garello, and M. A. Spirito, “Cooperative Spectrum Sensing based on the Limiting Eigenvalue Ratio Distribution in Wishart Matrices,” *IEEE Communications Letters*, vol. 13, no. 7, pp. 507–509, July 2009.

[7] F. Penna, R. Garello and M. A. Spirito, “Probability of Missed Detection in Eigenvalue Ratio Spectrum Sensing,” *2009 IEEE Int. Conf. on Wireless and Mobile Computing, Networking and Communications*, Marrakech, Morocco, 2009, pp. 117–122.

[8] L. Wei, and O. Trikkonenn, “Spectrum Sensing in the Presence of Multiple Primary Users,” *IEEE Transactions on Communications* , vol. 60, no. 5, pp. 1268–1277, Mar. 2012.

[9] M. F. Arts, *Eigenvalue-Based Spectrum Sensing for Cognitive Radio,* RWTH Aachen Phd Thesis, 2017.

[10] P. Bianchi, *et al.* “Performance of Statistical Tests for Source Detection using Random Matrix Theory,” *IEEE Transactions on Information Theory*, vol. 57, no. 4, pp. 2400–2419, Apr. 2011.

[11] S. N. Roy, “On a heuristic method of test construction and its use in multivariate analysis,” *Annals of Mathematical Statistics*, vol. 24, no. 2, pp. 220–238, 1953.

[12] H. Urkowitz, “Energy detection of unknown deterministic signals,” Proc. IEEE, vol. 55, no. 4, pp. 523–531, Apr. 1967.

[13] W. Zhang, R. K. Mallik, and K. B. Letaief, “Optimization of cooperative spectrum sensing with energy detection in cognitive radio networks,” *IEEE Transactions on Wireless Communications*, vol. 8, no. 12, pp. 5761-–5766, Dec. 2009.

[14] V. S. Muradi, R. K. Paithane, A. Ahmed and A. Pawar, “Spectrum sensing in cognitive radio using Labview and NI USRP,”, *2018 2nd International Conference on Inventive Systems and Control (ICISC)*, Coimbatore, India, 2018, pp. 1316-1319.

[15] A. Nafkha, M. Naoues, K. Cichon and A. Kliks, “Experimental spectrum sensing measurements using USRP Software Radio platform and GNU-radio,” *2014 9th International Conference on Cognitive Radio Oriented Wireless Networks and Communications (CROWNCOM)*, Oulu, Finland, 2014, pp. 429-434

[16] D. G. Riviello, G. Alfano, R. Garello, “Quadratic Forms in Random Matrices with Applications in Spectrum Sensing,” *Entropy: Special Issue Random Matrix Theory and Its Innovative Applications* vol. 27, no. 1, Jan. 2025.

[17] B. Nadler, "On the distribution of the ratio of the largest eigenvalue to the trace of a Wishart matrix," *Journal of Multivariate Analysis*, vol. 102, no. 2, pp. 363-371, Feb. 2011.
[18] O. Besson, and L. L. Scharf, "CFAR matched direction detector," *IEEE Transactions on Signal Processing*, vol. 54, no. 7, pp. 2840–2844, Jul. 2006.
[19] L. Wei, O. Tirkkonen, P. Dharmawansa, and M. R. McKay, "On the exact distribution of the scaled largest eigenvalue," *IEEE Int. Conf. Commun.*, Ottawa, ON, Canada, Jun. 2012.
[20] A. Kortun, M. Sellathurai, T. Ratnarajah and C. Zhong, "Distribution of the Ratio of the Largest Eigenvalue to the Trace of Complex Wishart Matrices," *IEEE Transactions on Signal Processing*, vol. 60, no. 10, pp. 5527-5532, Oct. 2012.
[21] B. Nadler, "On the distribution of the ratio of the largest eigenvalue to the trace of a Wishart matrix," *Journal of Multivariate Analysis*, vol. 102, no. 2, pp. 363–371, Feb. 2011.
[22] D. Féral, S. Péché, "The largest eigenvalues of sample covariance matrices for a spiked population: diagonal case," *Journal of Mathematical Physics*, vol. 50, no. 7, 2009.
[23] Z. D. Bai, "Methodologies in spectral analysis of large-dimensional random matrices, a review," *Statistica Sinica*, vol. 9, pp. 611-677, 1999.
[24] Ming Kang, and M.-S. Alouini, "Largest eigenvalue of complex Wishart matrices and performance analysis of MIMO MRC systems," *IEEE Journal on Selected Areas in Communications*, vol. 21, no. 3, pp. 418–426, April 2003.
[25] A. Zanella and M. Chiani, "On the Distribution of the ℓ-th Largest Eigenvalue of Spiked Complex Wishart Matrices," *Acta Physica Polonica B*, 2020
[26] Jinho Baik and Jack W. Silverstein, "Eigenvalues of large sample covariance matrices of spiked population models," *Journal of Multivariate Analysis*, vol. 97, no. 6, pp. 1382–1408, Jul. 2006.
[27] J. Baik, G. Ben Arous, G. and S. Péché, "Phase transition of the largest eigenvalue for non-null complex sample covariance matrices," *The Annals of Probability*, vol. 33 no. 5, pp. 1643–1697, 2005.
[28] M. Dieng, "Distribution functions for edge eigenvalues in orthogonal and symplectic ensembles: Painlevé representations," in *International Mathematics Research Notices*, vol. 2005, no. 37, pp. 2263-2287, 2005.